APPENDIX D. DIFFERENTIAL GPS TRUTHING

D.1 INTRODUCTION

A Differential GPS (DGPS) system was used as a truthing mechanism for assessing the range and range rate accuracies of forward-looking automotive radars, or other range, and range rate measurement systems, when the automobiles undergo dynamic maneuvers. The typical test scenario involves two vehicles, each equipped with GPS receivers. The primary vehicle was the ERIM testbed vehicle hosting the radar sensor under test. The secondary vehicle represented a typical vehicle that would be observed by the host vehicle during typical roadway driving. The proposed DGPS system provided an independent measurement of the "truth" trajectory, that is, the true range and range rate, between the primary and secondary vehicles. The proposed DGPS system must provide an accurate trajectory during vehicle accelerations in order to thoroughly assess the effects of vehicle dynamics on the radar signal. This appendix describes a test sequence to evaluate the accuracy of the proposed DGPS system during vehicle dynamics and demonstrates that such a system has sufficient accuracy for this application.

The truthing concept configuration consists of two vehicles equipped with GPS receivers that collect GPS data as the vehicles execute a test maneuver. At the same time, a basestation GPS located near the test site is also collecting GPS data. These data, which are intrinsically synchronized in time, are then processed off-line to produce an independent measurement of the range and range rate between the two test vehicles. Comparing the GPS-derived range and range-rate measurements with those produced by the radar sensor-under test provide an accurate assessment of the radar's range and range-rate measurement performance. This procedure was used during many of roadway tests conducted with the TRW FLAR sensor. Appendix F of this report contains a number of "GPS Range versus Radar Range" plots used to assess the performance of the FLAR sensor.

The post-processing of the GPS and radar data is performed by three software. The PNAV DGPS processing software is a commercial package provided by Ashtech. This software produces differentially corrected position and velocity data for each vehicle. These data are then processed by software developed by ERIM to produce the independent range and range-rate measurements of the vehicle pair. The final software module, also developed by ERIM, combines the two pairs of measurements to produce numerical and graphical comparisons of the data.

Before accepting the DGPS solution as a valid truthing mechanism, ERIM conducted experimental dynamic runs to assess the quality of the DGPS solution. These experiments were conducted with the ERIM Motion Measurement System (MMS). A high quality inertial navigation system, such as the MMS, can accurately measure relatively high frequency (that is, much greater than Schuler frequency) acceleration and can serve as the sensor to measure the "truth" trajectory during high dynamics if initial position and velocity errors are canceled. A high accuracy strapdown inertial navigation/Kalman filter algorithm is used to combine the DGPS position data with the inertial data to align the inertial platform and estimate the inertial navigation position and velocity errors and inertial sensor biases during periods of low vehicle dynamics. Prior to an applied acceleration or turn, the inertial navigation/Kalman filter algorithm is switched to the free inertial mode. In the free inertial mode the DGPS data is not applied to the inertial data, rather, the free inertial trajectory is calculated by integrating accelerometer data into inertial velocity and position. The free inertial trajectory is then compared with the DGPS trajectory during vehicle dynamics.

D.2 TRUTHING REQUIREMENTS

The performance requirements of vehicle-based radar systems vary depending upon the particular application (such as intelligent cruise control, lane change aid, forward collision warning, etc.). Table D-1 lists the proposed nominal requirements for an FCW system.

Table D-1. FCW System Performance Requirements

Measured Parameter	Performance
Range Accuracy	0.5 to 1 m
Range Rate Accuracy	0.3 to 1 m/s
Update Rate	10 Hz

These parameters relate to the required performance of the DGPS truthing system being proposed. A desirable truthing system would provide measurements of range and range rate that are an order of magnitude more accurate than the measurements of the system under test. The remainder of this appendix describes the results of a sequence of tests aimed at evaluating how well a DGPS system can meet the truthing system requirements.

DGPS performance can be categorized based on the combination of GPS observables which are combined to form the DGPS solution or trajectory. Five observables are available: the Coarse Acquisition or CA code on the L1 carrier frequency, the Precise or P code on the L1 carrier frequency, the P code on the L2 carrier frequency, the L1 carrier phase, and the L2 carrier phase. The carrier phase information can be continuously integrated to provide a fine measurement of change of range, or the rate of change of carrier phase can be used as a measure of range rate and used to smooth the code ranges. Three categories of DGPS performance were considered for the truthing system evaluation. The first category is a DGPS solution using all the observables with dual frequency continuously integrated carrier phase which requires a dual frequency receiver. The second category is a DGPS solution using the CA code and a single frequency carrier integrated phase. The third category is a DGPS solution using CA code with carrier smoothing. In general, the cost, complexity and performance decrease from the first to third categories.

D.3 DESCRIPTION OF TEST

The ERIM ITS testbed van is a 1994 Ford Club Wagon full-size van. The van has been modified to function as a data collection platform for evaluating radar-based and electro-optical-based automotive sensors. The instrumentation includes a Pentium-based PC, high-speed AD converters, video capture equipment, and supplemental environmental sensors.

Three 2-Hz GPS receivers were selected and installed in the van for the experiment. They included a Trimble 4000SE single frequency receiver, an Ashtech Z12 dual frequency receiver and an Ashtech DNS12 single frequency receiver. The three antennas were mounted on the roof of the van above the driver/passenger compartment area.

A 2 kilometer, roughly East/West, straight stretch of road with a 90 degree North bound turn at the East end served as the site for the experiment. An Ashtech Z12 ground reference receiver and a Trimble 4000SE ground reference receiver were set up on two known survey points approximately 150 meters from the 90 degree turn in the road. The Z12 ground reference receiver provides the differential correction for the Z12 and DNS12 rover receivers.

The following scenarios were selected for the experiment:

1. Maximum acceleration to a specified velocity, constant velocity for several seconds, then maximum braking to a stop;
2. High speed lane change;
3. Straight segment, 90 degree turn, then straight segment.

The maximum braking test represents a scenario in which the radar-equipped vehicle detects a leading vehicle in the same lane or adjacent lane that suddenly executes a panic stop. The lane change test represents a passing vehicle suddenly moving into the same lane ahead of the radar-equipped vehicle (i.e., a rapid "cut-in"). The hard turn test represents an radar-equipped vehicle that must track and sort vehicles and roadside targets while heading into and through a turn.

The ERIM Motion Measurement System (MMS) provides the reference or truth data for the evaluation of the DGPS system during high acceleration. The MMS, described in Reference D-2, was originally developed to provide highly accurate trajectory measurement of the airborne platforms used in the formation of inverse SAR imagery. It consists of a Honeywell H770 RLG INS modified to provide outputs of delta-theta and delta-velocity at 1200 Hz, a Datum 9250-5730 Time/Frequency Reference (atomic clock), and appropriate control and recording electronics. Some of the significant sensor error specifications are listed in Table D-2. As an example, an accelerometer bias of 50 micro-g would result in an position error of 24 millimeters after 10 seconds. An accelerometer scale factor error of 100 parts/million and an applied acceleration of 0.75 g for 4 seconds would result in a position error of 6 millimeters. The gyro error contributions are at least an order of magnitude less for these same time periods. Extensive testing, described in Reference D-2, has verified the performance of the INS. The MMS has been used in several other SAR programs. The MMS has recently been installed in the van where it was used to record the motion of the van for a SAR experiment involving ground moving target detection. The INS was mounted on the floor of the van, approximately in the center of the cargo area. The atomic clock provides the time tagging for the inertial data. The atomic clock is synchronized to GPS time by means of its own internal GPS receiver.

Table D-2. MMS Inertial Sensor Error Specifications

Error Source	Specification
Accelerometer Bias	50 ug
Accelerometer Scale Factor	100 ppm
Gyro Drift	0.007 deg/hr
Gyro Random Walk	0.002 deg/rt-hr

All data from the inertial navigation unit, the GPS receivers and the reference GPS receivers were recorded for post processing. The Ashtech data was processed using Ashtech PNAV software, the Trimble data was processed with both Trimble POSTNAV II and FLYKIN software. GPS data was processed to create several DGPS trajectories of position and velocity. Each trajectory covers the duration of the day's experiment. Several trajectories could be created from each receiver pair. For example, the Ashtech Z-12 data was processed to produce trajectories using several combinations of observables, including All Observables, CA Code plus L1 Carrier Integrated Phase, and CA Code with Carrier Smoothing. By selecting subsets of the five observables available in the Z12 data the second two trajectories can be created and used to emulate single frequency receivers. The advantage of the emulation of the single frequency receivers is to compare the three categories of trajectories with data recorded from the same rover antenna and L1 pre-amplifier. The single frequency DNS12 data and

Trimble 4000SE data were processed to provide trajectories using CA Code plus L1 Carrier Integrated Phase, and CA Code with Carrier Smoothing

The inertial data was processed with the Advanced Navigation Processor (ANP), a high accuracy strapdown navigation/Kalman filter algorithm developed under the MMS program. The ANP uses the 1200 Hz delta-theta and delta-velocity data to provide a 50 Hz navigation trajectory output of position, velocity, and attitude. The ANP Kalman filter is processed at a 1 Hz rate. The ANP Kalman filter can use position data from any of the DGPS trajectories to align the inertial platform and estimate the inertial system errors (this process is called aiding). The lever arm vectors from the INS reference point to the phase center of each GPS antenna were carefully measured. In the ANP, the position measurements from the selected DGPS trajectory are translated to the INS reference point for use in the ANP Kalman filter calculations. The 50 Hz inertial trajectory is translated back to the selected GPS antenna point for direct comparison to the DGPS trajectory. All DGPS and ANP trajectories for this experiment were referenced to a rectangular coordinate frame which is centered at the survey point occupied by the Ashtech ground reference receiver, with x-axis aligned with East, y-axis with North, and z-axis with the Up or vertical direction.

The experiment began with the set-up of the ground reference receivers. After positioning the receiver antennas over the survey points, data logging to laptop computers was initiated. The equipment in the van was turned on several minutes before the test began in order to allow enough time prior to the first run for the MMS to align. Each run executes one of the three scenarios described in the introduction. Data was collected continuously for the duration of the experiment. After several minutes of stationary data had been collected, the driver began the first run. A few minutes of stationary data collection was planned between each run to allow several minutes of data between each maneuver for inertial alignment. Data was collected on two days, July 9, 1996 (GPS day 191), and July 11, 1996 (GPS day 193).

The inertial data was initially processed to create one trajectory for the duration of the day's experiment. The beginning of each dynamic maneuver was identified from the inertial position, velocity, and attitude trajectories. The time for the beginning of the free inertial trajectory for each dynamic maneuver was selected to be approximately 1-2 seconds prior to the beginning of the maneuver. The inertial data and corresponding DGPS position data was then reprocessed in the ANP for each maneuver. The beginning of the aided portion of each ANP trajectory was selected to include at least four minutes of data prior to the free inertial time and long enough to include a 180 degree turn of the van/platform in order to refine the Kalman filter estimates of some of the inertial error states such as the accelerometer bias states and the platform tilt error states.

D.4 RESULTS

The results presented in this appendix come from the July 11 experiment; the data presented is from the Ashtech Z-12 receiver. All GPS data is referenced to the same rover antenna. Three DGPS trajectories are presented, including: all observables (labeled "0 All Observables"), CA Code plus L1 Carrier Integrated Phase (labeled "X CA Code+Integrated Carrier"), and CA Code with Carrier Smoothing (labeled "+ CA Code w/ Smoothing"). The time scale on each plot is referenced to the beginning of free inertial mode. The Ashtech DGPS trajectories were processed using both the automotive dynamics and aircraft dynamics selection in PNAV. No significant differences were evident between the two dynamics modes. The DGPS trajectories described in this paper were processed with the aircraft dynamics mode. The ANP Kalman filter used the All Observables DGPS position for the aided inertial mode.

The first series of plots come from Run 1, Eastbound maximum braking. The van was moving at a speed of approximately 45 m.p.h., 20 meters/sec, when a panic stop was initiated. Figure D-1 shows a 10 second span of the East position; Figure D-2 shows the corresponding East velocity data. From the inertial velocity data, the braking begins at approximately t = 1.2s and ends at about t = 4.5s. The rocking motion of the van on its suspension can be seen in the inertial velocity data from about t = 4.5s to t = 6s. At t = 6s the driver had released the brake and begun to slowly pull off to the side of the road (due to occasional traffic on the road). Note that the CA Code with Carrier Smoothing has a significant overshoot in position and velocity. Figures D-3 and D-4 show East position and velocity with an expanded time scale. The CA Code with Carrier Smoothing trajectory reaches a maximum error of 2.5 meters in position and velocity errors of 7 m/s relative to the inertial trajectory. The All Observables and the CA Code with Carrier Integrated Phase trajectory positions follow the inertial position closely. There is a bias of 0.25 meter between the All Observables and the CA Code with Carrier Integrated Phase trajectories, which is probably due to the difference in the number of observables used in the solution. The All Observables and the CA Code with Carrier Integrated Phase velocities are nearly identical and both exhibit a time lag relative to the inertial data.

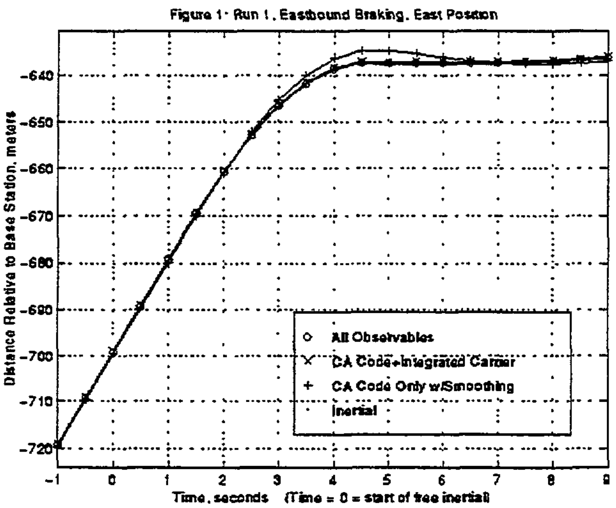

Figure D-1. Run 1, Eastbound Braking, East Position

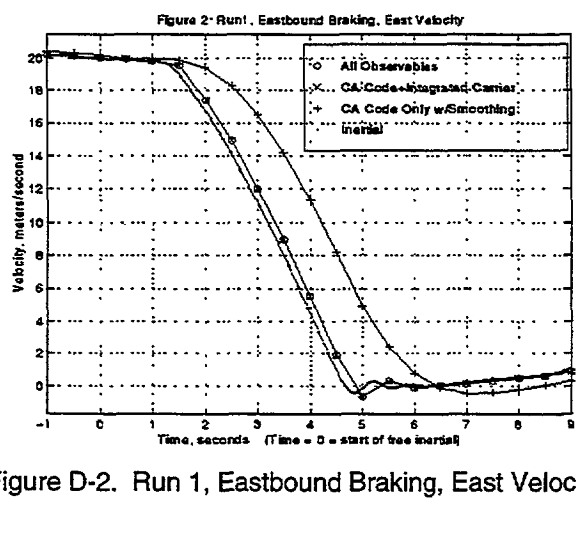

Figure D-2. Run 1, Eastbound Braking, East Velocity

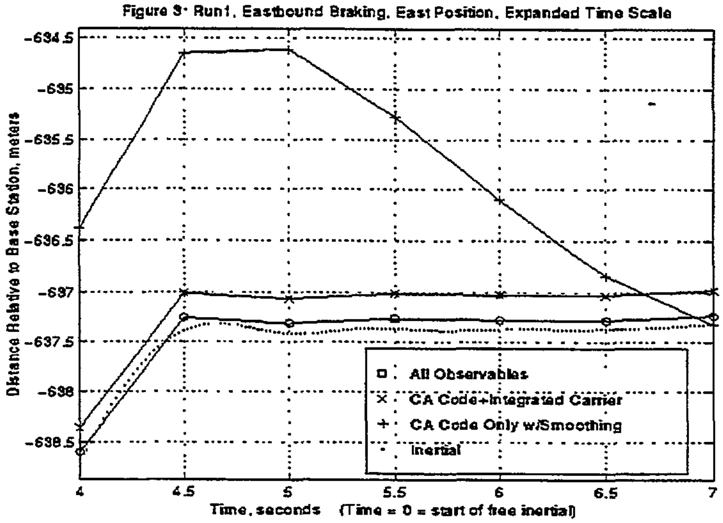

Figure D-3. Run 1, Eastbound Braking, East Position, Expanded Time Scale

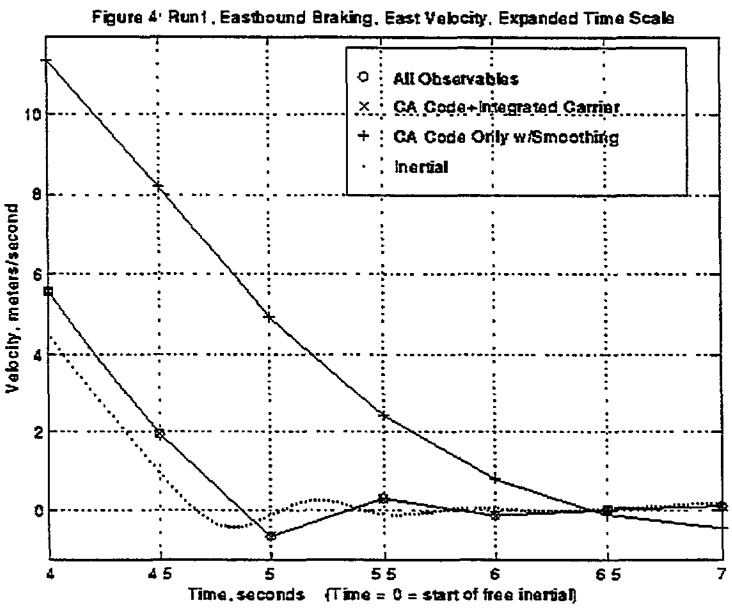

Figure D-4. Run 1, Eastbound Braking, East Velocity, Expanded Time Scale

Figure D-5 shows the Up position for the Eastbound Braking, Run 1. The plot shows that there could be a noticeable difference in DGPS trajectories using All Observables and one using the CA Code and a single frequency Carrier Integrated Phase. This example shows a difference of 1.75 meters. The CA Code with Carrier Smoothing position trajectory shows a curious response which can be more easily seen in the velocity data in Figure D-6. This velocity trajectory reaches a peak of 0.3 m/s vertical velocity. The vertical velocity of the other DGPS solutions appear to follow the inertial data with the same data lag observed in the horizontal velocity. As a side note, the slight negative velocity seen in the vertical velocity while the van is still moving is real. According to the local terrain survey data, the road is not level; it decreases in elevation about 3 meters going from West to East over the 2 kilometer stretch.

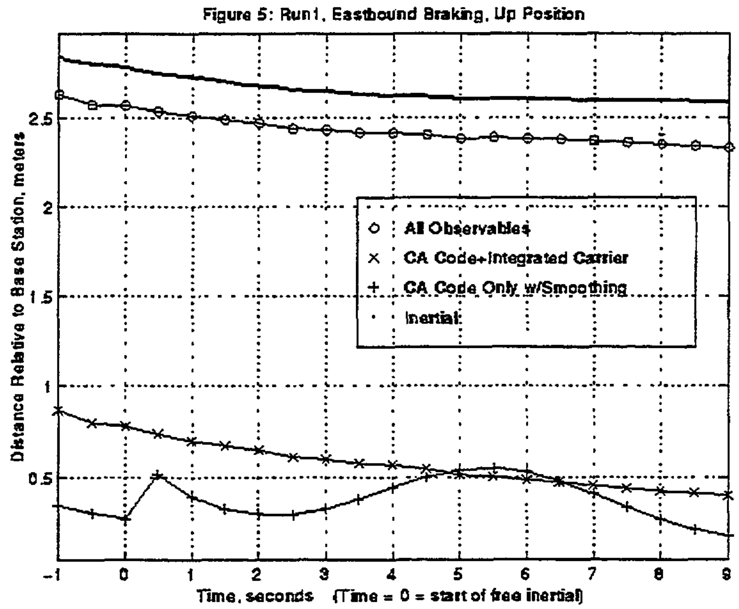

Figure D-5. Run 1, Eastbound Braking, Up Position

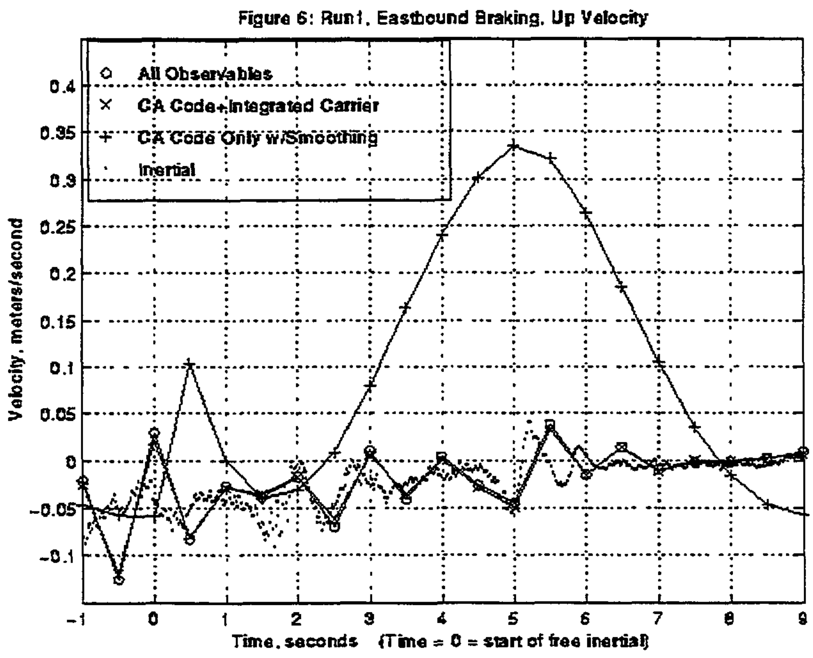

Figure D-6. Run 1, Eastbound Braking, Up Velocity

The next series of plots come from Run 3, the Eastbound Lane Change. Figure D-7 shows the North position, once again showing that a bias exists between the All Observables and the CA Code with Carrier Integrated Phase trajectories. The data indicates that the road is not precisely East/West. Figure D-8 shows the North velocity. In this plot, it can be seen that the sudden lane change is too fast for the filter in the CA Code with Carrier Smoothing trajectory. Figures D-9 and D-10 show the North position and velocity with an expanded time scale. The DGPS solutions using continuously integrated carrier phase follow the dynamics closely, with the All Observables solution exactly following the free inertial solution and the CA Code with Carrier Integrated Phase solution showing about a 0.9 meter bias relative to the free inertial trajectory.

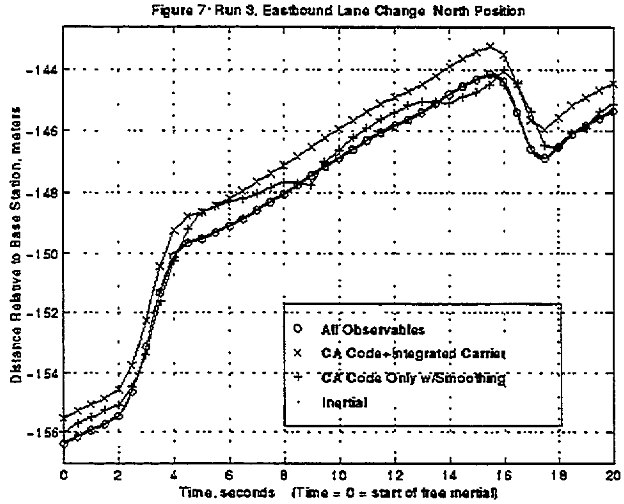

Figure D-7. Run 3, Eastbound Lane Change, North Position

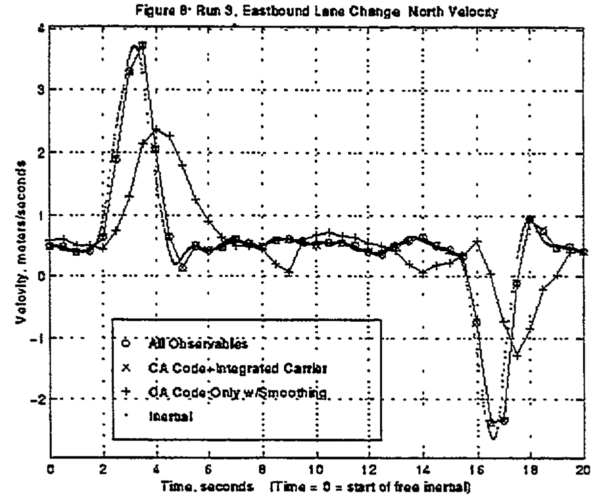

Figure D-8. Run 3, Eastbound Lane Change, North Velocity

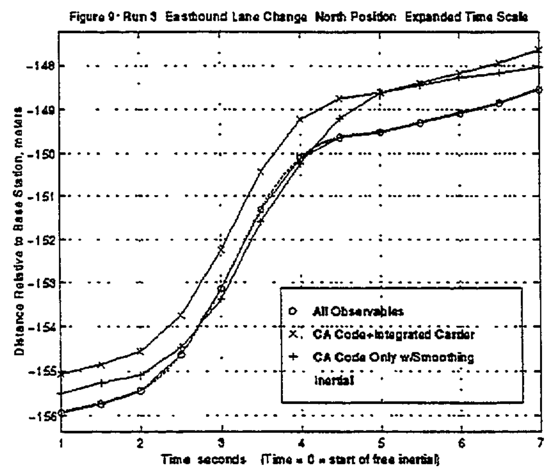

Figure D-9. Run 3, Eastbound Lane Change, North Position, Expanded Time Scale

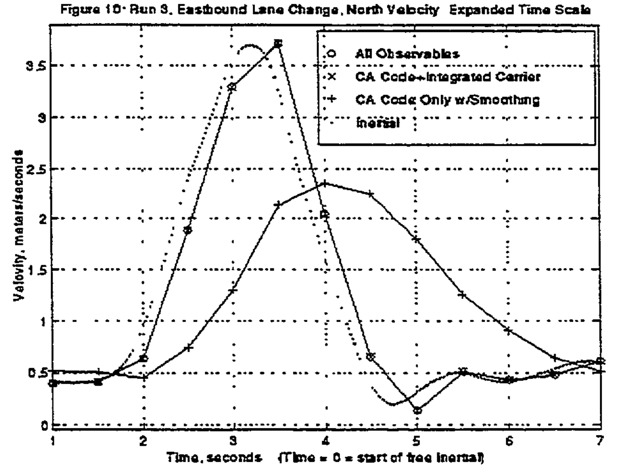

Figure D-10. Run 3, Eastbound Lane Change, North Velocity, Expanded Time Scale

The next series of plots come from Run 6, the East to North turn. Figures D-11 and D-12 show the East and North position while Figures D-13 and D-14 show the East and North velocity. At the beginning of free inertial time, t = 0s, the van is slowing and begins to brake prior to the turn at t = 4s. The van is in the turn from about t = 7s to t = 12s, as can be seen from the velocity data. At t = 12s the van is out of the turn and begins accelerating back up to 20 meters/second. Once again, the data shows that the CA Code with Carrier Smoothing has errors on the order of a few meters in position and several meters/second relative to the inertial data during the turn. The All Observables and CA Code with Carrier Integrated Phase trajectories show good response during the turn in comparison to the inertial data.

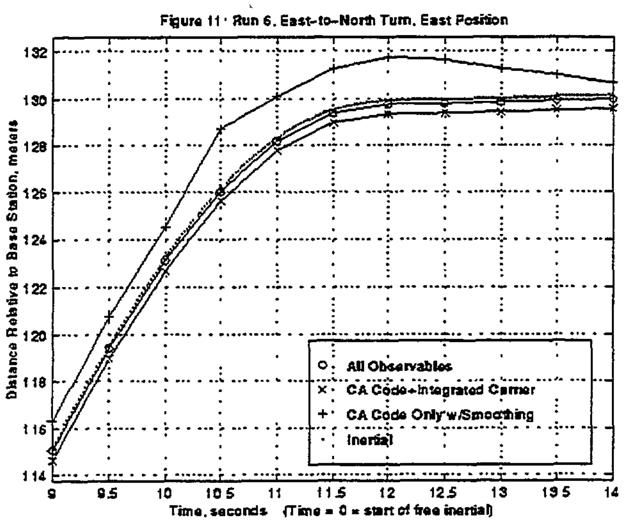

Figure D-11. Run 6, East-to-North Turn, East Position

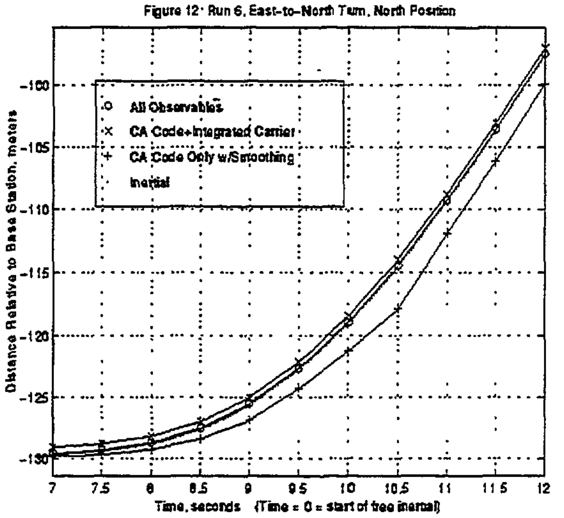

Figure D-12. Run 6, East-to-North Turn, North Position

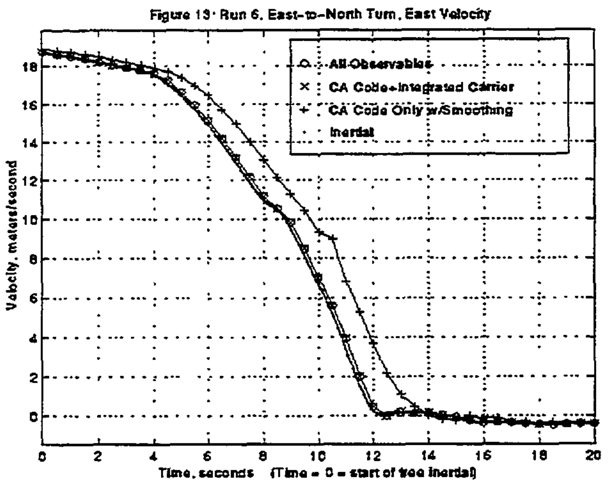

Figure D-13. Run 6, East-to-North Turn, East Velocity

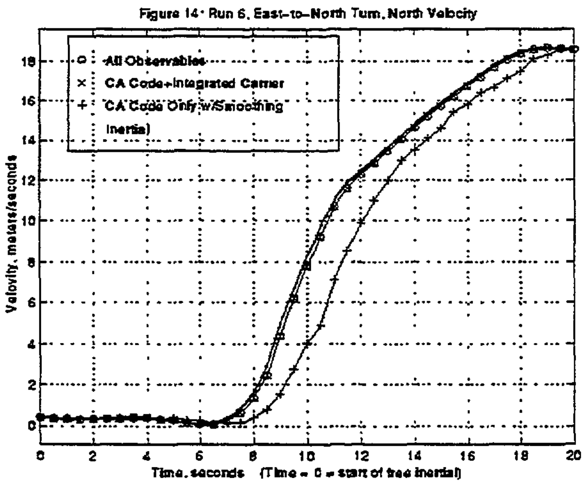

Figure D-14. Run 6, East-to-North Turn, North Velocity

D.5 CONCLUSIONS

The data presented in this appendix are obtained from the same Ashtech Z-12 rover receiver and processed in different combinations of observables to represent dual frequency carrier integrated phase DGPS solution, a CA Code with single carrier integrated phase DGPS solution, and a CA Code only with carrier smoothing solution. In this manner, the results are all referenced to the same rover antenna. The DNS-12 receiver and the Trimble 4000SE receiver are both single frequency receivers. The data from those receivers were processed to obtain trajectories corresponding to the CA Code with Carrier Integrated Phase and CA Code with Carrier Smoothing. After correcting for the different lever arm vectors from the inertial reference point and the phase center of the other two antennas, results similar to the CA Code with Integrated Phase and CA Code with Carrier Smoothing were obtained. This shows that the emulation of these systems is valid and the conclusions are also valid.

The DGPS solutions using continuously integrated carrier phase observables have been shown to significantly improve accuracy relative to CA Code with Carrier Smoothing during the scenario dynamics. This is when radar signals from FCW systems will exhibit significant range, range rate, and Doppler modulation. By continuously integrating the DGPS carrier phase, the DGPS solution accurately follows the dynamics expected for the FCW radar system evaluation. This can be understood by realizing that the continuously integrated phase measurement is a delta-position or integrated velocity measurement that is similar to the delta-velocity measurement obtained by an inertial navigation system.

The selection of a single frequency receiver that is capable of continuously integrated carrier phase DGPS offers cost savings over a dual frequency receiver. However, the testing demonstrated that noticeable position errors can exist in the single frequency solution. The continuously integrated carrier phase observables provide a fine measurement of change of position, but the CA code and the two P code measurements provide an estimate of the integer ambiguities inherent in the carrier phase measurements and help control the residual absolute position error if used in a complementary filter implementation. It seems reasonable that the standard deviation of that residual position error is larger for the single frequency solution using only the CA code observable. Also, the time to reach an accurate estimate of the integer ambiguities can be significantly longer for the single frequency receiver because it does not have the benefit of the wide-lane ambiguity processing that is available with two frequency data. Figure D-15 shows an example of the settling time of the dual frequency carrier integrated phase solution and the single frequency carrier integrated phase solution. The plot shows the North position of the van in which the van began moving 135 seconds after data recording was initiated. The CA Code with Carrier Integrated Phase solution differs by approximately 1 meter relative to the All Observables solution while the van is still stationary. Once the van begins moving, the error relative to the All Observables solution reaches as much as 5 meters. The solutions appear to converge after several minutes of data. A single frequency DGPS solution would require a programmed settling time built into each FCW evaluation test each time data-logging is initiated. The dual frequency receiver system can reduce this time to a minimum and also reduce the time needed to reacquire and correct for cycle slips after the periods of signal blockage that can be expected in a ground vehicle application. A dual frequency receiver using differential carrier integrated phase processing with all observables would contribute to increased efficiency and simpler operation of the truthing system in the FCW radar evaluations.

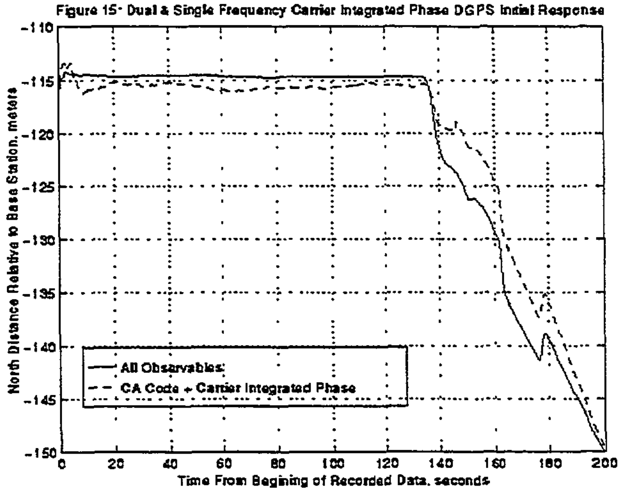

Figure D-15. Dual and Single Frequency Carrier Integrated Phase DGPS Initial Response

D.6 ACKNOWLEDGMENTS

This project was sponsored by ERIM through its Internal Research and Development funds. This appendix is an edited version of the paper "Dynamic Testing of a DGPS System used as a Truthing

Mechanism for Collision Avoidance Radar Evaluation," authored by John W. Sisak and Paul K. Zoratti. The paper was presented at The Institute of Navigation's National Technical Meeting in San, Jose, CA, 14-16 January 1997. The authors wish to thank all their ERIM colleagues who contributed effort to this project. In particular, the authors wish to thank Tom Blessing, Bob Hrabec, Eric Batzdorfer and Tom Chaplin for equipment installation, site preparation, and assistance during the test. Thanks also go to William Hanna, Mike Harrison, and Tom McQuade for their help in processing the inertial data and GPS data.

D.7 REFERENCES

D-1. "System and Parametric Trade-Offs of Forward Looking Automotive Radar Systems," Walter Nagy, Joseph Wilhelm, IEEE 1996 National Radar Conference, Ann Arbor MI, 13-16 May, 1996.

D-2. "High Accuracy, Short Term Trajectory Measurement of an Airborne Vehicle for Control of Inverse Synthetic Aperture Radar Image Formation," John W. Sisak & members of the ERIM Staff, 16th Biennial Guidance Test Symposium, Holloman AFB, NM, 5-7 October, 1993.